Molecular Crystals and Liquid Crystals

ISSN: 1542-1406 (Print) 1563-5287 (Online) Journal homepage: http://www.tandfonline.com/loi/gmcl20

Cubic Phase Magnetic Nanoparticles

Seung Kyeong Hong & Jin-Chul Kim

To cite this article: Seung Kyeong Hong & Jin-Chul Kim (2015) Cubic Phase Magnetic Nanoparticles, Molecular Crystals and Liquid Crystals, 607:1, 123-134, DOI: 10.1080/15421406.2014.939602

To link to this article: http://dx.doi.org/10.1080/15421406.2014.939602

Mol. Cryst. Liq. Cryst., Vol. 607: pp. 123–134, 2015

ISSN: 1542-1406 print/1563-5287 online
DOI: 10.1080/15421406.2014.939602

Cubic Phase Magnetic Nanoparticles

SEUNG KYEONG HONG AND JIN-CHUL KIM*

Department of Medical Biomaterials Engineering, College of Biomedical Science and Institute of Bioscience and Biotechnology, Kangwon National University, Chuncheon, Kangwon-do, Korea

Fe^{2+}/Fe^{3+} salt-containing cubic phases were prepared by hydrating the molten monoolein (MO)/stearic acid (SA) with the iron ions solution. Optically isotropic cubic phases and phase transition temperature of cubic phase having a series of different MO/SA ratio were obtained. Cubic phase nanoparticles (so-called cubosomes) containing iron oxide nanoparticles (IONs) were prepared. The saturation magnetization of cubosomal IONs was lower than that of IONs prepared in bulk phase. Iron ions chemically deteriorated MO of cubic phase 30 days after stored at room temperature, indicating that ION-containing cubosomes should be prepared soon after iron ions-containing cubic phase is formed.

Keywords Cubic phase nanoparticles; magnetic nanoparticle; phase transition

Introduction

Magnetic nanoparticles (MNPs) have been studied for their applications in the field of diagnosis therapy. There are three kinds of magnetic nanoparticles, namely, metallic, bimetallic, and superparamagnetic iron oxide nanoparticles (SPIONs). Among them, iron oxide nanoparticle (ION) is the most widely used in the medical applications including in vivo medical imaging [1–3], drug delivery [4–7], tissue repair [8], and hyperthermia [9–11] applications because it is non-toxic to human body, readily prepared, and reactive with ligands, imaging molecules, and therapeutic ones, and it exhibits good magnetic property [12–17]. ION is classified into magnetite (Fe_3O_4) and maghemite (γ-Fe_2O_3) depending on its composition, and the former one is more commonly used because of its better magnetic property [18, 19]. The co-precipitation of Fe^{2+}/Fe^{3+} salt solution is usually adopted to prepare ION because the method is simple and requires no toxic compounds [20, 21]. The method of loading of therapeutic agents into ION is the covalent attachment on the surface or the entrapment in the coating of the surface, so the amount of the payload is small and limited. Furthermore, the procedure for the covalent attachment of ligands and pharmaceutical agents to the surface of ION is somewhat complicated and it can deteriorate the ligands and the pharmaceutics. In order to circumvent these shortcomings, ION-loaded cubic phase nanoparticles (CPN) (ION-CPN) were prepared by micronizing ION-loaded

*Address correspondence to Jin-Chul Kim, Department of Medical Biomaterials Engineering, College of Biomedical Science and Institute of Bioscience and Biotechnology, Kangwon National University, 192-1, Hyoja 2 dong, Chuncheon 200-701, Kangwon-do, Korea. Tel.: +82 33 250 6561; Fax: +82 33 25 9 5645. E-mail: jinkim@kangwon.ac.kr

Color versions of one or more of the figures in the article can be found online at www.tandfonline.com/gmcl.

cubic phase lump in an excess aqueous phase, where ION-loaded cubic phase lump was prepared by alkalizing cubic phase lump containing the precursor ions (Fe^{2+}/Fe^{3+}) with NaOH solution. Small and uniform ION could be formed in the cubic phase because the precipitation will take place in the water channel. And, not only hydrophilic drugs but also lipophilic ones can be loaded in ION-CPN because the water channel together with lipid matrix constitutes CPN. Furthermore, much more amount of pharmaceutical agents could be loaded in ION-CPN than in ION itself, due to the high vacancy in CPN. However, ION was formed only in the utmost layer of cubic phase lump, not throughout the lump when the cubic phase containing the iron ions was alkalized. This is because the IONs formed in the utmost layer can block the penetration of alkali solution into the cubic phase and prevent the cubic phase being alkalized. As a result, ION-CPNs prepared by micronizing the ION-loaded cubic phase lump would be different from one another in its composition. In order to avoid this problem, ION was prepared in this study in CPN, not in cubic phase lump. Due to the small diameter of CPN, the alkali solution will diffuse throughout the nanoparticle. In addition, stearic acid (a negatively charged lipid) was included in CPN to prevent the leak-out of iron ions from the CPN into an aqueous bulk phase. A brief description for the preparation of ION-CPN is as follows. Monoolein and stearic acid were co-melted in a vial immersed in a hot water, a warmed aqueous solution of Fe^{2+}/Fe^{3+} salt was layered over the melt, and it was allowed to stand at room temperature until a clear gel (cubic phase lump) is formed. And then an excess amount of water was added to the cubic phase lump contained in a vial, and the cubic phase lump was micronized into CPN using a homogenizer. Owing to an electrostatic interaction between the iron ions (Fe^{2+}/Fe^{3+}) and the fatty acid, the leak-out of the ions from CPN into bulk aqueous phase can be prevented. Then, a concentrated alkali solution (NaOH solution) was added to the suspension of Fe^{2+}/Fe^{3+}-loaded CPN for the formation of ION in the CPN. The schematic diagram for the preparation of ION-CPN is depicted in Scheme 1.

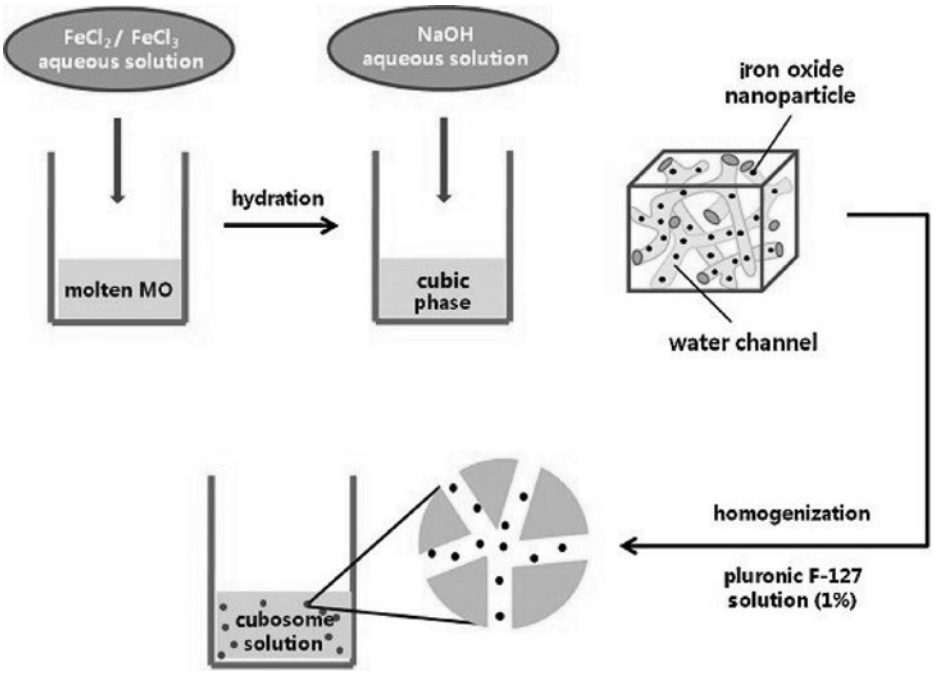

Scheme 1. Schematic diagram for preparation of ION-CPN.

Experiment Details

Materials

Iron(II) chloride tetrahydrate ($FeCl_2 \cdot 4H_2O$, 99.0%), iron(III) chloride hexahydrate ($FeCl_3 \cdot 6H_2O$, 97%), sodium hydroxide (NaOH, 98%), and Pluronic F-127 were purchased from Sigma-Aldrich Chemical Co. (St. Louis, MO, USA). Monoolein (Monomuls 90-O 18) was gifted by Cognis Ltd. (Hardley, Hampshire, UK). All other reagents were in analytical grade.

Preparation of Iron Ions-Containing Cubic Phases

MO and SA were put in 10 ml of vials so that the molar ratio was 100:0, 99.75:0.25, 99.5:0.5, 99:1, 98:2, 96:4, 92:8, and 84:16 and the total mass (MO plus SA) was 2 g. In parallel, iron chloride (II) tetrahydrate ($FeCl_2 \cdot 4H_2O$) and iron chloride (III) hexahydrate ($FeCl_3 \cdot 6H_2O$) were dissolved in distilled water so that the concentration was 0.006 M and 0.012 M, respectively. MO and SA were melted together in a water bath kept at 65°C, and then 0.667 ml of the iron ions solution was layered carefully over the molten lipids. The two phase system was allowed to stand around 25°C until the iron ions solution was completely adsorbed and gel was formed (it took about 10 days). As a control, the same amount of distilled water containing no iron ions was layered over molten MO for the preparation of MO cubic phase containing no iron ions. The iron ions-containing gels of which MO/SA ratio is 100:0, 99.75:0.25, 99.5:0.5, 99:1, 98:2, 96:4, 92:8, and 84:16 will be termed Gel(100:0), Gel(99.75:0.25), Gel(99.5:0.5), Gel(99:1), Gel(98:2), Gel(96:4), Gel(92:8), and Gel(84:16), respectively. And MO cubic phase containing no iron ions will be termed CuPhaNii.

Optical Microscopy

The textures of MO gels were observed on a polarizing microscope (CX31, OLYMPUS, Japan). MO gel was put in the space between two cover glasses spaced by 100 μm thick poly(ethylene terephthalate) films. MO gel was heated at a rate of 3°C/min in a hot stage (FP82, Mettler) equipped with a temperature controller (FP80HT, Mettler). The photos of gel images were taken in the temperature range of 25°C–70°C.

Preparation of ION-Containing Cubic Phase Nanoparticles

0.5 g of iron ions-containing cubic phase (e.g., Gel(100:0), Gel(99.75:0.25), Gel(99.5:0.5), Gel(99:1)) was put in a 10 ml vial, and 5 ml of Pluronic F-127 solution (0.5%) in distilled water was added to the cubic phase. The cubic phases were micronized for 10 min in a tip type sonicator (VC 505–VC 750, SONICS) with pulse-on for 30 sec and pulse-off for 30 sec. 0.3 ml of NaOH solution (0.048M) was added to the cubosomal suspensions and then they were allowed to stand at 25°C for 48 hr for the formation of ION within the cubosomes. In parallel, CuPhaNii (MO cubic phase containing no iron ions) was also micronized under the same condition. The cubosomes prepared from Gel(100:0), Gel(99.75:0.25), Gel(99.5:0.5), and Gel(99:1) will be termed ION-CPN(100:0), ION-CPN(99.75:0.25), ION-CPN(99.5:0.5), and ION-CPN(99:1). And the cubosome prepared from CuPhaNii will be abbreviated to CuboNii.

Characterization of ION-Containing Cubosomes

The mean diameter and the size distribution of CuboNii and ION-CPNs were determined on a dynamic light scattering machine (90 Plus, Brookhaven Instrument Corporation). The suspensions of ION-CPNs and CuboNii were diluted with distilled water so that the count per second was 50–200. The TEM photos of ION contained in ION-CPNs were taken on a transmission electron microscope (LEO 912AB OMEGA, Germany, at KBSI (Chuncheon, Korea)). The magnetization hysteresis loops of CuboNii and ION-CPNs were obtained at a room temperature on a magnetometer (#73002, Lake Shore Cryotroni, USA, in the Central Laboratory Center of Kangwon National University).

^{1}H NMR Study for Chemical Stability of Monoolein Against Iron Ions

Gel(100:0) was allowed to stand at room temperature for 30 days. The gel was freeze-dried, the residue was washed in distilled water to remove iron ions and the washed lipid was freeze-dried. The dried lipid was dissolved in $CDCl_3$ for ^{1}H NMR spectroscopy (Bruker DPX 400 MHz Karlsruhe, Germany, in the Central Laboratory Center of Kangwon National University). In parallel, monoolein was also subjected to the ^{1}H NMR spectroscopy.

Colorimetric Study for Chemical Stability of Monoolein Against Iron Ions

Gel(100:0), Gel(99.75:0.25), Gel(99.5:0.5), and Gel(99:1) were allowed to stand at room temperature for 30 days. The gels were freeze-dried, the residues were washed in distilled water to remove iron ions and the washed lipids were freeze-dried. The dried lipids put in an aluminum pan (Tzero pan), and the thermograms were obtained on a differential scanning calorimeter (DSC Q2000, TA Instruments, USA, in the Central Laboratory Center of Kangwon National University) in the temperature range of 10°C–50°C at the heating rate of 2°C/min. In parallel, the thermogram of MO was also taken as a control.

Results and Discussion

Preparation of Iron Ions-Containing Cubic Phases

Figure 1 shows the photos of CuPhaNii, Gel(100:0), Gel(99.75:0.25), Gel(99.5:0.5), Gel(99:1), Gel(98:2), Gel(96:4), Gel(92:8), and Gel(84:16). CuPhaNii, which comprises MO and distilled water containing no iron ions, was optically transparent. The optical

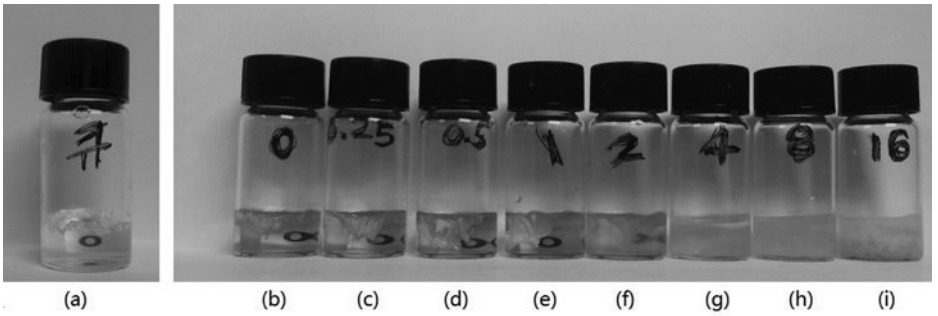

Figure 1. Photos of CuPhaNii (a), Gel(100:0) (b), Gel(99.75:0.25) (c), Gel(99.5:0.5) (d), Gel(99:1) (e), Gel(98:2) (f), Gel(96:4) (g), Gel(92:8) (h), and Gel(84:16) (i).

transparency indicates that cubic phase was successfully formed, because the cubic phase is optically isotropic [22–24]. MO has the packing parameter slightly greater than 1 and it is known to form a cubic phase when it was hydrated with an adequate amount of aqueous solution [25–27]. Gel(100:0), which is composed of MO and iron ions solution, also was optically transparent. Iron chloride (II) tetrahydrate ($FeCl_2 \cdot 4H_2O$) and iron chloride (III) hexahydrate ($FeCl_3 \cdot 6H_2O$) are water soluble, so they will exist in the water channel of cubic phase and hardly affect the effective packing parameter of MO. Thus, the iron ions (Fe^{2+}/Fe^{3+}) will not interfere with the formation of cubic phase. On the other hand, Gel(99.75:0.25), Gel(99.5:0.5), and Gel(99:1) were also transparent. So it can be said that SA can be included in MO cubic phase without disrupting the structure when the ratio of MO/SA was equal to and less than 99:1. However, Gel(98:2), Gel(96:4), Gel(92:8), and Gel(84:16) were turbid, indicating that cubic phase could hardly be formed when the ratio of MO/SA was equal to and greater than 98:2. SA is oil-soluble so it will be intercalated into MO lipid matrix and may have a significant effect on the effective packing parameter of MO. Thus, the inclusion of SA in the MO gel preparation may lead to non-cubic phases. In fact, MO cubic phase could accommodate an oil-soluble compound (e.g., Triclosan and Hinokitiol) only in a small quantity without losing its structure [28–31].

Optical Microscopy

Figure 2 shows the polarizing photomicrographs of Gel(100:0), Gel(99.75:0.25), Gel(99.5:0.5), Gel(99:1), Gel(98:2), Gel(96:4), Gel(92:8), and Gel(84:16) at different temperatures. CuPhaNii, which comprises MO and distilled water containing no iron ions, exhibited a clean texture and no birefringence when the temperature was less than 58°C, indicating that CuPhaNii is a cubic phase below the temperature. Since cubic phase is optically transparent, it is known to show no birefringence [7]. The gel began to exhibit birefringence at 58.4°C. MO cubic phase was reported to undergo a thermal phase transition to a reversed hexagonal phase at a certain temperature [32]. The birefringence observed

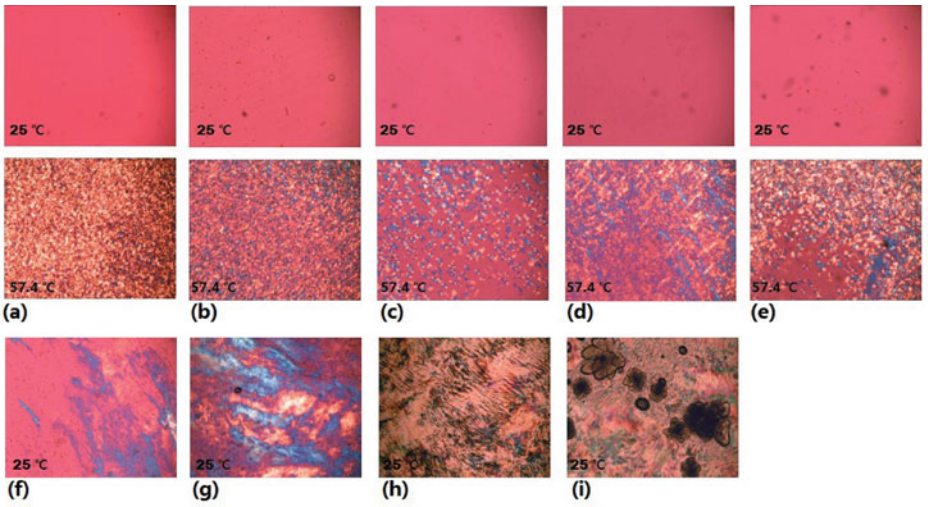

Figure 2. Polarized photomicrographs of CuPhaNii (a), Gel(100:0) (b), Gel(99.75:0.25) (c), Gel(99.5:0.5) (d), Gel(99:1) (e), Gel(98:2) (f), Gel(96:4) (g), Gel(92:8) (h), and Gel(84:16) (i) at different temperatures.

at the higher temperature is because the hexagonal phase is not optically isotropic. In our previous study, MO cubic phase where hydrogen peroxide was contained in the aqueous phase in its water channel began to show its birefringence around 62°C [33]. Gel(100:0), which composed of MO and an iron ions aqueous solution also showed a clean texture and no birefringence either when the temperature was less than 58°C, and the gel began to exhibit birefringence at 58.1°C. That is, the temperature where birefringence began to appear was not markedly different between two kinds of cubic phases. Iron ions will be contained in the water channels of MO cubic phase and they seem to have little effect on the phase transition of lipidic MO matrix. As Gel(100:0) did, Gel(99.75:0.25), Gel(99.5:0.5), and Gel(99:1) exhibited no birefringence below their phase transition temperatures but they exhibited birefringence above the temperatures. The temperature where Gel(99.75:0.25), Gel(99.5:0.5), and Gel(99:1) began to show birefringence was around 57.4°C, 54.7°C, and 50.0°C, respectively. That is, the phase transition temperature decreased with increasing the content of SA. SA would disrupt the crystalline structure of MO cubic phase so it may fluidize the lipidic crystalline matrix, leading to a decreased phase transition temperature. On the other hand, Gel(98:2), Gel(96:4), Gel(92:8), and Gel(84:16) exhibited birefringence even at a room temperature (25°C) where the gels were prepared. It means that cubic phase could be hardly formed when the content of SA was greater than or equal to 2%. SA could inhibit the packing of MO cubic phase when it is included in the preparation at a certain level, because SA is lipid-soluble and it will be intercalated in MO matrix. In fact, only a little amount of oil-soluble ingredients (e.g., Triclosan and Hinokitiol) could be accommodated in MO cubic phase without disrupting the structure [29, 31, 34, 35].

Characterization of ION-Containing Cubosomes

Figure 3 shows the size distributions of CuboNii and ION-CPN(100:0), ION-CPN(99.75:0.25), ION- CPN(99.5:0.5), and ION- CPN(99:1). Monomodal distributions were observed in all the preparations tested. And the mean diameter of CuboNii, ION-CPN(100:0), ION-CPN(99.75:0.25), ION-CPN(99.5:0.5), and ION-CPN(99:1) was around 270 nm, 190 nm, 200 nm, 195 nm, and 205 nm, respectively. The size of ION-CPNs was significantly less than that of CuboNii. Iron oxide will be precipitated-out within cubic phase so the iron oxide precipitates can disturb the crystal structure of the cubic phase. As a result, mechanical strength of cubic phase containing the precipitate will be less than that of empty cubic phase. So cubic phases containing the precipitates can be more readily micronized, leading to smaller particles.

Figure 4 shows the TEM photos of CuboNii, ION-CPN(100:0), ION-CPN(99.75:0.25), ION-CPN(99.5:0.5), ION-CPN(99:1), and iron oxide particles prepared in a bulk phase. No trace of particles was observed on the photo of CuboNii. Particles were observed on the photo of ION-CPNs and they are believed to be iron oxide particles. When electron beam was irradiated to the replica, it will readily go through the area free of iron oxide particles but it will scatter on iron oxide particles due to the high atom density of iron. Iron oxide particles shown on the photos were less than 10 nm in diameter in all ION-CPNs. Iron ions (Fe^{2+}/Fe^{3+}) are water-soluble and they will exist in the water channel of ION-CPNs. Upon alkalizing the suspensions of ION-CPNs, the iron ions will co-precipitate to form iron oxide particles in the water channels. As a result, the size of the iron oxide particles would be comparable with the size of the water channel (ca. 5 nm). On the other hand, iron oxide particles prepared in a bulk phase was more than 30 nm in diameter and they were found to be in agglomerates. The co-precipitation in bulk phase imposes no steric

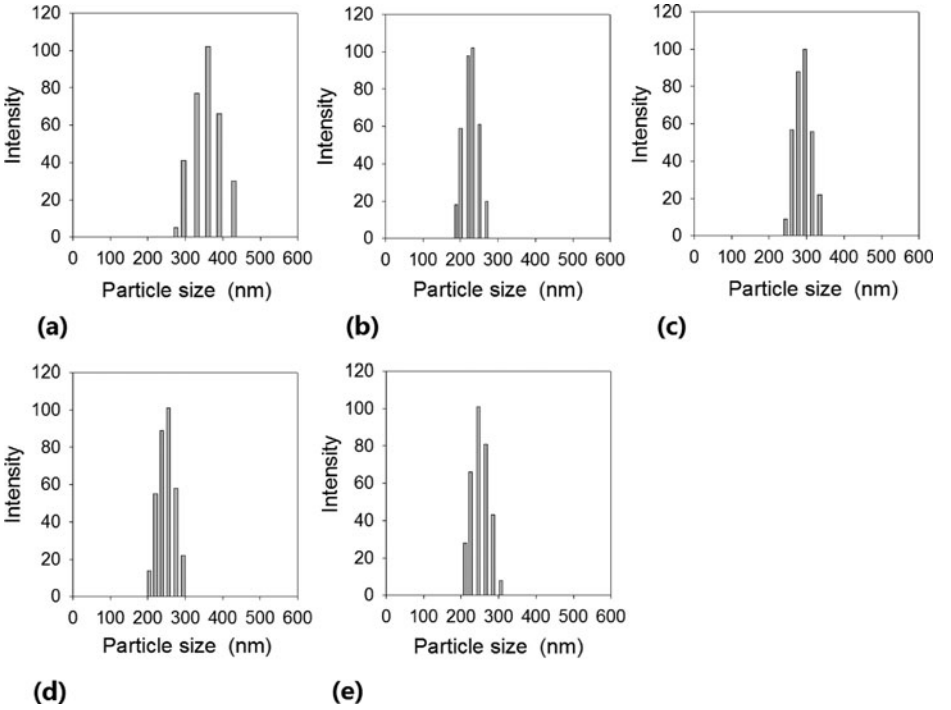

Figure 3. Size distributions of CuboNii (a) and ION-CPN(100:0) (b), ION-CPN(99.75:0.25) (c), ION-CPN(99.5:0.5) (d), and ION-CPN(99:1) (e).

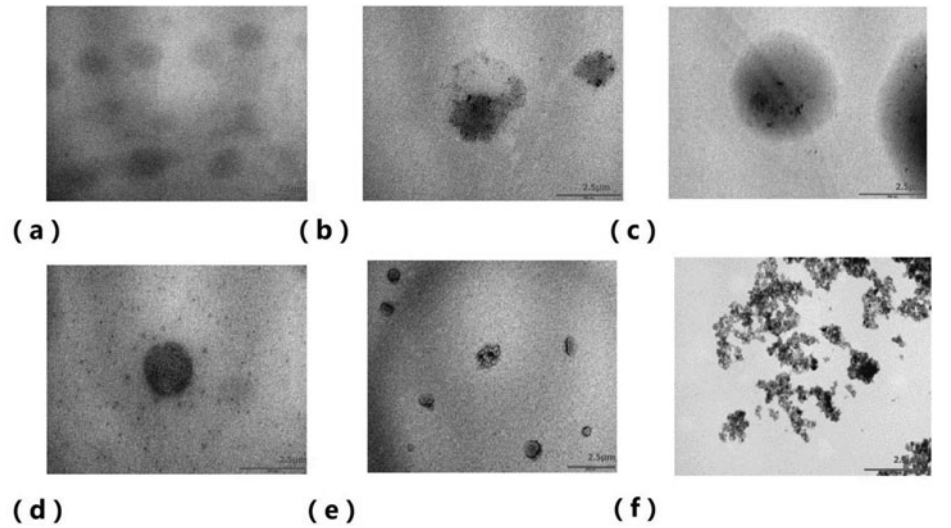

Figure 4. TEM photos of CuboNii (a), ION-CPN(100:0) (b), ION-CPN(99.75:0.25) (c), ION-CPN(99.5:0.5) (d), ION-CPN(99:1) (e), and iron oxide particles prepared in a bulk phase (f).

Table 1. M_s, M_r, and H_c of ION-CPN(99:1) and ION prepared in bulk phase

	ION	ION-CPN(99:1)
Saturation magnetization (M_s)	50.3 emu/g	5.4 emu/g
Remanent magnetization (M_r)	5.4 emu/g	0.9 emu/g
Coercivity (H_c)	207.4 Oe	377.9 Oe

hindrance on the growth of iron oxide particles, so the method will allow for the formation of larger particles. The water channel of ION-CPNs is believed to act as a nano-reactor for the formation of iron oxide particles.

Figure 5 shows the magnetization hysteresis loops of CuboNii, ION-CPN(100:0), ION-CPN(99.75:0.25), ION-CPN(99.5:0.5), ION-CPN(99:1), and iron oxide particles prepared in a bulk phase. CuboNii showed no magnetization because it has no iron oxide in its structure. Neither ION-CPN(100:0) nor ION-CPN(99.75:0.25) nor ION- CPN(99.5:0.5) showed a significant magnetization. However, ION-CPN(99:1) exhibited a marked magnetization. ION-CPN(99:1) will capture iron ions more than ION- CPN(100:0), ION-CPN(99.75:0.25), and ION-CPN(99.5:0.5), because of its more negative charge point. Thus, iron oxide will be formed in the former ION-CPN more than in the latter ION-CPNs. ION prepared in a bulk aqueous phase showed a stronger magnetization. The magnetic property of IONs is characterized by saturation magnetization (M_s), remanent magnetization (M_r), and coercivity (H_c). The M_s, M_r, and H_c of ION-CPN(99:1) and ION prepared in bulk phase were summarized in Table 1. The IONs prepared in the present study are believed to be ferromagnetic because the values of H_c and M_r were not zero. The M_s of ION-CPN(99:1) was much smaller than that of ION prepared in bulk phase, possibly because cubosome can shield ION from the magnetic field.

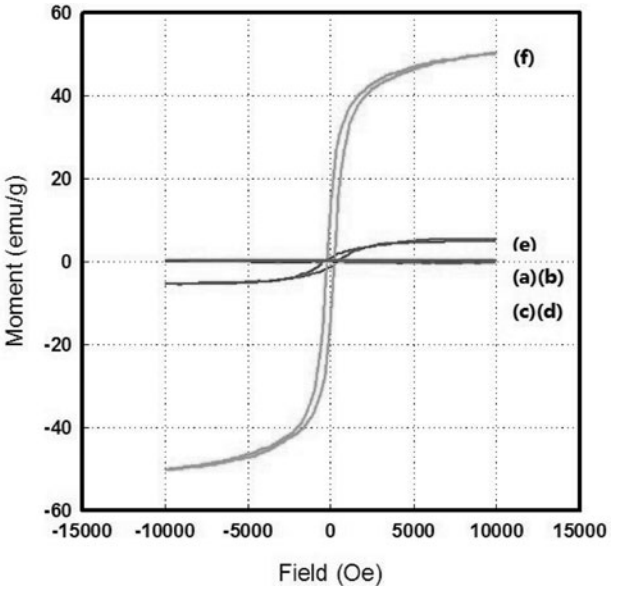

Figure 5. Magnetization of CuboNii (a), ION-CPN(100:0) (b), ION-CPN(99.75:0.25) (c), ION-CPN(99.5:0.5) (d), ION-CPN(99:1) (e), and iron oxide particles prepared in a bulk phase (f).

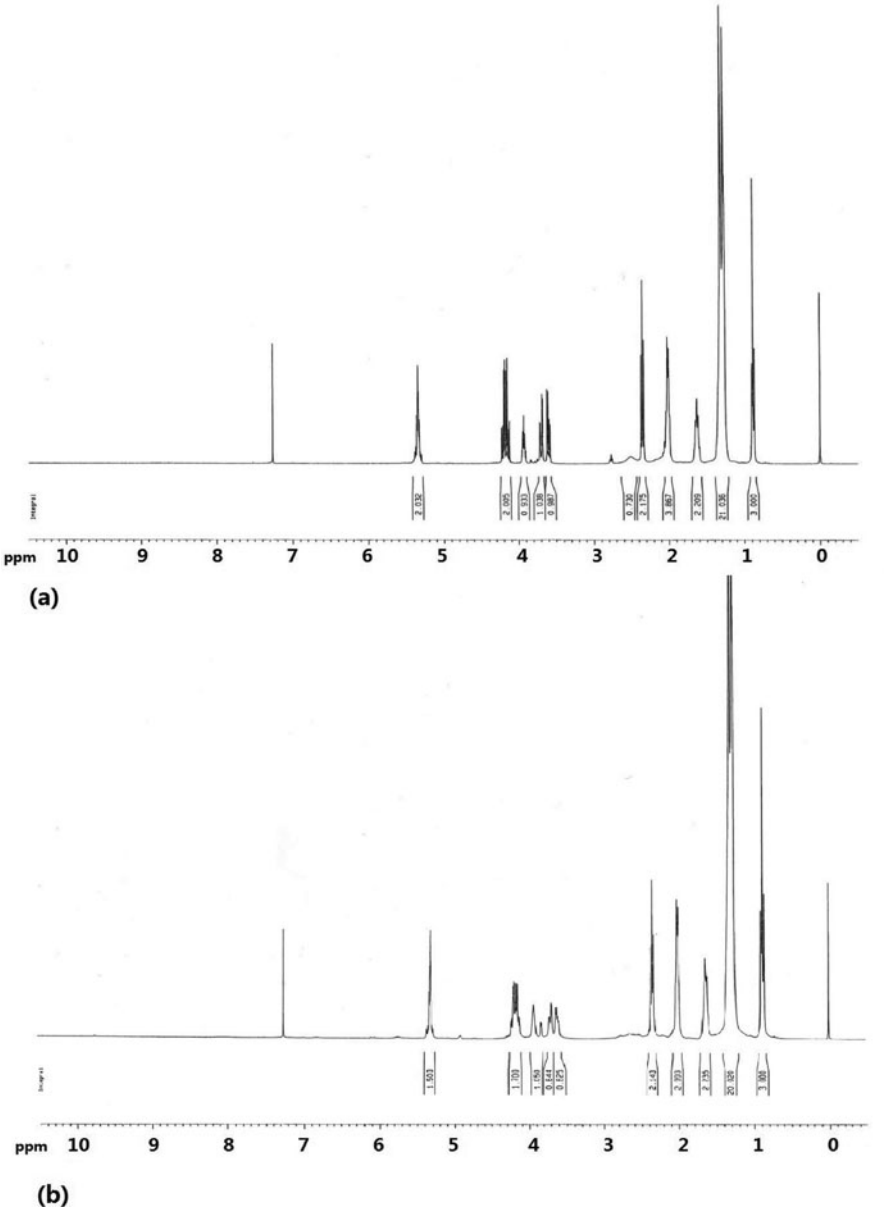

Figure 6. NMR spectra of MO(a) and lipid of Gel(100:0) (b) after stored at room temperature for 30 days.

^{1}H NMR Study for Chemical Stability of Monoolein Against Iron Ions

Figure 6 shows the NMR spectra of MO and the lipid of Gel(100:0), which was allowed to stand at room temperature for 30 days. $-CH_3$ was found at 0.88 ppm, $-(CH_2)_{11}-$ of hydrocarbon chain at 1.25 ppm, $-CH_2-CH_2-COO-$ at 1.55 ppm, $-CH_2-C=C-$ at 2.02 ppm, $-CH_2-COO-$ at 2.32 ppm, glycerol $-CH_2$ adjacent to ester bond at 3.63 ppm, glycerol $-CH$ at 3.90 ppm, and glycerol $-CH_2$ adjacent to hydroxyl group at 4.20 ppm. In

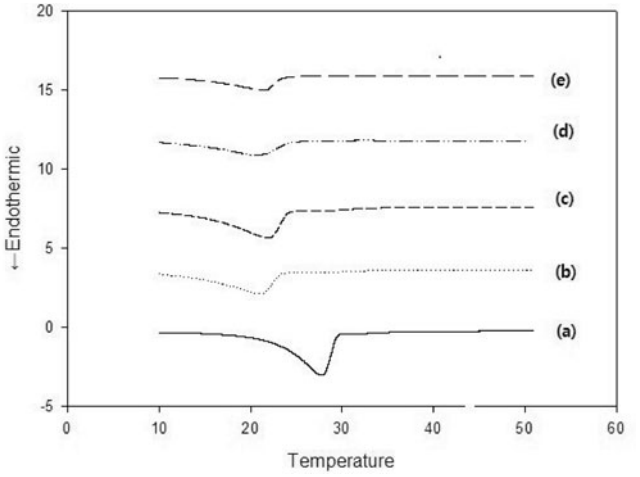

Figure 7. Thermograms of MO (a) and lipid of Gel(100:0) (b), Gel(99.75:0.25) (c), Gel(99.5:0.5) (d), and Gel(99:1) (e) after stored at room temperature for 30 days.

the ^{1}H NMR spectrum of MO, the peak area ratio of $-CH_3/-HC=CH-$ was 3/2.02, close to theoretical value of 3/2. In the ^{1}H NMR spectrum of lipid of Gel(100:0), the peak area ratio was 3/1.5, indicating that approximately 25% of double bond was disappeared. Iron ions contained in Gel(100:0) seem to oxidize the double bond.

Colorimetric Study for Chemical Stability of Monoolein Against Iron Ions

Figure 7 shows the thermograms of MO and the lipids of Gel(100:0), Gel(99.75:0.25), Gel(99.5:0.5), and Gel(99:1), which were allowed to stand at room temperature for 30 days. MO exhibited an endothermic peak around 28°C, due to the melting. The melting point of MO was reported to be 35°C. The reason that the observed melting point was lower than the reported one is the purity of MO used in the present study was 90%. Di- and tri-glycerides, and the mono-glycerides of different hydrocarbons are contained as impurity. The lipid of the gels exhibited an endothermic peak around 21°C, much lower than the melting point of MO, and the position of the peak was almost the same whichever the gel was. As described previously, iron ions can oxidize MO of cubic phase (Fig. 6), so it could make MO chain be shortened. The molecular debris produced from MO can deteriorate the crystalline structure thus they are thought to be responsible for why the melting point of the gel lipid was lower than that of MO.

Conclusion

ION-containing cubosomes were prepared by micronizing Fe^{2+}/Fe^{3+} salt-containing cubic phases and co-precipitating Fe^{2+}/Fe^{3+} salt in the water channels of the cubosomes. SA was included in the preparation of cubosomes to prevent the leakage of iron ions. SA could be interacted into MO cubic phase without disrupting the structure when MO/SA ratio was less than or equal to 99:1. The inclusion of iron ions had little effect on the phase transition temperature of cubic phases. But, the inclusion of SA had a significant effect on the phase transition temperature. The phase transition temperature decreased from 58°C to 50°C when SA/MO ratio increased from 0:100 to 1:99. This is possibly because SA will be

intercalated in lipidic MO matrix so it can fluidize the matrix. The mean diameters of ION-containing cubosomes were 180–200 nm and the values were less than the mean diameter of cubosomes free of ION (ca. 270 nm). ION seemed to disturb the intermolecular interaction of MO so ION-containing cubic phase will be readily micronized into smaller particles. On TEM photos, IONs in cubosomes were less than 10 nm in diameter and they were smaller than IONs prepared in bulk phase. The water channel of cubosome is believed to act as a nano-reactor for the formation of ION. The IONs prepared in the present study exhibited magnetization hysteresis loops, indicating that they were ferromagnetic. Cubosomal ION exhibited a lower saturation magnetization than ION prepared in bulk phase did, possibly because cubosome shields ION from magnetic field. MO of cubic phases containing the iron ions underwent oxidation 30 days after stored at room temperature, indicating that ION-containing cubosomes should be prepared soon after iron ions-containing cubic phase is formed.

Acknowledgment

Following as results of a study on the "Leaders in Industry-university Cooperation" Project, supported by the Ministry of Education, Science & Technology (MEST) and the National Research Foundation of Korea (NRF).

References

[1] Wickline, S. A., Neubauer, A. M., Winter, P. M., Caruthers, S. D., & Lanza, G. M. (2007). *J. Magn. Reson. Imag.*, *25*, 667.
[2] Yoo, M. K. *et al.* (2008). *J. Nanosci. Nanotechnol*., *8*, 5196.
[3] Alexiou, C., Jurgons, R., Sellger, C., & Iro, H. (2006). *J. Nanosci. Nanotechnol.*, *6*, 2762.
[4] Chavanpatil, M. D., Khdair, A., & Panyam, J. (2006). *J. Nanosci. Nanotechnol.*, *6*, 2651.
[5] Mukesh, U., Kulkani, V., Tushar, R., & Murthy, R. S. R. (2009). *J. Biomed. Nanotechnol.*, *5*, 99.
[6] Laurent, S., Bontry, S., Mahien, I., Elst, L. V., & Muller, R. N. (2009). *Curr. Med. Chem.*, *16*, 4712.
[7] Shah, J. C., Sadhale, Y., & Chilukuri, D. M. (2001). *Adv. Drug Deliv. Rev.*, *47*, 229.
[8] Šponarová, D. *et al.* (2011). *J. Biomed. Nanotechnol*., *7*, 384.
[9] Thomas, L. A. *et al.* (2009). *J. Mater. Chem.*, *19*, 6529.
[10] Lee, J. S. *et al.* (2011). *J. Nanosc. Nanotechnol.*, *11*, 4153.
[11] Psimadas, D. *et al.* (2011). *J. Biomed. Nanotechnol.*, *8*, 575.
[12] Jain, T. K., Morales, M. A., Sahoo, S. K., Leslie-Pelecky, D. L., & Labhasetwar, V. (2005). *Mol. Pharm.*, *2*, 194.
[13] Chertok, B. *et al.* (2008). *Biomaterials*, *29*, 487.
[14] Zhang, L. *et al.* (2008). *Pharmacol. Ther.*, *83*, 761.
[15] Buyuhatipoglu, K., Miller, T. A., & Clyne, A. M. (2009). *J. Nanosci. Nanotechnol.*, *9*, 6834.
[16] Babic, M. *et al.* (2008). *Bioconjugate Chem.*, *19*, 740.
[17] Gupta, A. K., & Gupta, M. (2005). *Biomaterials*, *26*, 3995.
[18] Vatta, L. L., Sanderson, R. D., & Koch, K. R. (2006). *Pure Appl. Chem. 78*, 1793.
[19] Roh, Y., Vali, H., Phelps, T. J., & Moon, J. W. (2006). *J. Nanosci. Nanotechnol.*, *6*, 3517.
[20] Kwon, T. K., & Kim, J. C. (2011). *Drug Dev. Ind. Pharm.*, *37*, 56.
[21] Gupta, A. K., & Curtis, A. S. G. (2004). *Biomaterials*, *25*, 3029.
[22] Pevzner, S., & Regev, O. (2000). *Micropor. Mesopor. Mat.*, *38*, 413.
[23] Mann, A. K. *et al.* (2008). *J. Nanosci. Nanotechnol.*, *8*, 6290.
[24] Carvalho, F. C. *et al.* (2012). *J. Biomed. Nanotechnol.*, *8*, 280.
[25] Kim, J. C. *et al.* (2004). *Colloids Surf. B: Biointerfaces*, *36*, 161.

[26] Caboi, F. *et al.* (2001). *Chem. Phys. Lipids*, *109*, 47.
[27] Tolbert, S. H. *et al.* (2001). *Chem. Mater.*, *13*, 2247.
[28] Kwon, T. K., Hong, S. K., & Kim, J. C. (2012). *J. Ind. Eng. Chem.*, *18*, 563.
[29] Kwon, T. K., & Kim, J. C. (2010). *J. Dispersion Sci. Technol*., *31*, 1004.
[30] Kwon, T. K. *et al.* (2010). *Colloid. J.*, *72*, 205.
[31] Kim, J. C. *et al.* (2004). *Colloids Surf. B: Biointerfaces*, *36*, 161.
[32] Fraser, S., Separovic, F., & Polyzos, A. (2009). *Eur. Biophys. J.*, *39*, 83.
[33] Petri-Fink, A., de Lausanne, E. P. F., & Hofmann, H. (2007). *IEEE Trans. Nanobiosci.*, *6*, 289.
[34] Kwon, T. K., & Kim, J. C. (2010). *Int. J. Pharm.*, *392*, 268.
[35] Leesajakul, W., Nakano, M., Taniguchi, A., & Handa, T. (2004). *Colloids Surf. B: Biointerfaces*, *34*, 253.